

# Crystallization Region, Crystal Growth, and Phase Transitions of $\text{KNd}(\text{PO}_3)_4$

I. Parreu, R. Solé, Jna. Gavaldà, J. Massons, F. Díaz, and M. Aguiló\*

*Física i Cristallografia de Materials, Universitat Rovira i Virgili, Imperial Tarraco, 1, 42005 Tarragona, Spain*

*Received September 2, 2003. Revised Manuscript Received October 24, 2003*

We determined the crystallization region of  $\text{KNd}(\text{PO}_3)_4$  (KNP), the isotherms of saturation temperature, and three neighboring phases of this crystallization region,  $\text{NdPO}_4$ ,  $\text{Nd}(\text{PO}_3)_3$ , and  $\text{NdP}_5\text{O}_{14}$ , in the  $\text{Nd}_2\text{O}_3\text{--K}_2\text{O--P}_2\text{O}_5$  system. We successfully grew KNP single crystals by the top seeded solution growth slow cooling method (TSSG). To optimize the growth process solution composition, seed orientation and rotation velocity were analyzed. We studied the evolution with the temperature of the KNP cell parameters in the room temperature to 773 K range, and the linear thermal expansion tensor of KNP was studied. We also studied the phase transitions of KNP in the room temperature to 1273 K range and found an irreversible decomposition at 1165 K. The second harmonic efficiency measured was at least similar to that of  $\text{KH}_2\text{PO}_4$  (KDP).

## Introduction

As a Nd stoichiometric laser material,  $\text{KNd}(\text{PO}_3)_4$  (KNP) is potentially useful for miniature laser devices because it strongly absorbs the pumping light in short distances (50–100  $\mu\text{m}$ ).<sup>1</sup> This high absorption efficiency is allowed in stoichiometric laser materials by the high active ion concentration. Materials for miniature Nd lasers should have two structural characteristics: first, they should have no local inversion symmetry about the  $\text{Nd}^{3+}$  ions so as not to decrease the probability of radiative transitions, and second, the Nd–O polyhedrons should be isolated among them so as to decrease the quenching fluorescence process of  $\text{Nd}^{3+}$  ions. The structure of KNP satisfies both of these crystallographic conditions.<sup>1</sup> When we solved the structure of KNP by single-crystal diffraction analysis,<sup>2</sup> we obtained a similar result that had been reported in 1975. The monoclinic structure of KNP has  $P2_1$  as space group, with cell parameters,  $a = 7.2860(10)$  Å,  $b = 8.4420(10)$  Å,  $c = 8.0340(10)$  Å,  $\beta = 92.170(10)^\circ$ ;  $Z = 2$ ;  $V = 493.80(11)$  Å<sup>3</sup>.

Several Nd-stoichiometric laser materials have so far been reported. Of these, two representative Nd-stoichiometric phosphates are  $\text{NdP}_5\text{O}_{14}$ <sup>3–5</sup> and  $\text{LiNd}(\text{PO}_3)_4$  (LNP);<sup>6–8</sup> both of them satisfied the structural conditions already mentioned. However, KNP has a struc-

tural advantage over these other Nd-stoichiometric phosphates: it has an acentric space group ( $P2_1$ ). The fact that the structure of KNP does not have a center of inversion may allow nonlinear optical processes,<sup>9</sup> such as second-harmonic generation.

The aim of this paper is to study and optimize the conditions of the KNP crystal growth process and perform the basic structural characterization of the material.

Therefore, as information in the literature is poor and sometimes confused, we determined the crystallization region of KNP in the self-flux and phase transitions of KNP. Some papers on the growth of KNP single crystals can be found in the literature,<sup>1,10</sup> but they do not contain much information. On the other hand, they reported the incongruent melting of KNP decomposing into  $\text{Nd}(\text{PO}_3)_3$  and  $\text{KPO}_3$  at 1155 K,<sup>10</sup> a thermal arrest at 1153 K related to a crystalline-to-amorphous transition and a monoclinic-to-orthorhombic transition at 440 K.<sup>1</sup> However, neither of these transitions is well documented.

We also dedicated so many efforts to determine the morphology of KNP, since it is essential to orient and polish the samples for later physical characterizations.

Finally, we performed some physical characterizations of the material, such as linear thermal expansion tensor and second harmonic generation.

## Experimental Section

**KNP Crystallization Region.** To determine the concentration region and crystallization temperatures of KNP in the  $\text{Nd}_2\text{O}_3\text{--K}_2\text{O--P}_2\text{O}_5$  system, we studied several solution compositions. The procedure we used for each solution composition study is summarized in the following four steps: solution preparation and homogenization, determination of the saturation temperature, crystal growth, and phase identification.

\* To whom correspondence should be addressed. E-mail: aguilo@quimica.urv.es.

(1) Hong, H. Y.-P. *Mater. Res. Bull.* **1975**, *10*, 1105.  
 (2) Parreu, I.; Solans, X.; Aguiló, M. Unpublished.  
 (3) Weber, H. P.; Damen, T. C.; Danielmeyer, H. G.; Tofield, B. C. *Appl. Phys. Lett.* **1973**, *22*, 534.  
 (4) Danielmeyer, H. G.; Huber, G.; Krühler, W. W.; Jeser, J. P. *Appl. Phys.* **1975**, *2*, 335.  
 (5) Chinn, S. R.; Pierce, J. W.; Heckscher, H. *IEEE J. Quantum Electron.*, to be published.  
 (6) Otsuka, K.; Yamada, T. *Appl. Phys. Lett.* **1975**, *26*, 311.  
 (7) Chinn, S. R.; Hong, H. Y.-P. *Appl. Phys. Lett.* **1975**, *26*, 649.  
 (8) Otsuka, K.; Yamada, T.; Saruwatari, M.; Kimura, T. *IEEE J. Quantum Electron.* **1975**, *QE-11*, 330.

(9) Xue, D.; Zhang, S. *Phys. Status Solidi* **1998**, *165*, 509.

(10) Mazurak, Z.; Jezowska-Trzebiatowska, B.; Schultze, D.; Wąligora, C. *Cryst. Res. Technol.* **1984**, *19*.

Table 1. Growth Data for KNP Single Crystals

expt	solution composition Nd <sub>2</sub> O <sub>3</sub> -K <sub>2</sub> O-P <sub>2</sub> O <sub>5</sub>	solution wt (g)	seed orientation	rotation velocity (rpm)	cooling interval (K)	cryst dimens (a × b × c)(mm <sup>3</sup> )	cryst wt (g)
1	10/30/60	20	c*	45	12		
2	10/30/60	20	b	45	16	7.3 × 2.6 × 10.0	0.37
3	10/30/60	20	a*	45	17	3.4 × 9.5 × 8.0	0.30
4	10/30/60	20	a*	60	17	4.2 × 10.6 × 8.3	0.33
5	7/31/62	20	a*	60	17	3.0 × 7.9 × 5.9	0.34
6	4/31/65	20	a*	60	24.5	2.7 × 9.05 × 7.3	0.27
7	6/34/60	20	a*	60	16	3.0 × 9.1 × 6.8	0.36
8	6/34/60	20	b	60	15	8.4 × 4.4 × 6.3	0.41
9	6/34/60	20	a*	75	15	3.5 × 9.3 × 6.9	0.47
10	6/34/60	20	b	75	15	11.8 × 2.8 × 7.2	0.47
11	6/34/60	200	a*	75	17	7.8 × 14.9 × 9.5	1.84
12	6/34/60	200	b	75	17	16.0 × 6.2 × 12.7	1.98

The experiments were carried out in a vertical tubular furnace with a Kantal AF heater. The temperature was measured by an S-type thermocouple and controlled by an EUROTHERM 818 P controller/programmer connected to a thyristor. Platinum crucibles (25 cm<sup>3</sup>) were used to prepare roughly 20 g of solution, using Nd<sub>2</sub>O<sub>3</sub>, K<sub>2</sub>CO<sub>3</sub>, and NH<sub>4</sub>H<sub>2</sub>PO<sub>4</sub> mixed at the chosen ratios. To prevent the formation of phosphate acids, which can react with platinum at high temperatures, these initial reagents were decomposed by heating them at the minimum temperature required to reach the complete bubbling of NH<sub>3</sub>, CO<sub>2</sub>, and H<sub>2</sub>O. The solution was then homogenized by maintaining the temperature at about 1173–1273 K for 5–12 h, depending on the solution composition.

Small KNP crystals were then added to the solution. Because of the surface tension and natural convection processes, these crystals stayed on the center of the surface, which was the coldest point of the whole solution. Then, the saturation temperature was accurately determined by observing the growth or dissolution of these small crystals over long periods of time. A platinum disk with a rotation of 45 rpm placed into contact with the solution surface was then used to grow the crystals by lowering the solution temperature to about 25 K below its saturation temperature. The cooling rate used to obtain the supersaturation of the solution was 1–2 K/h.

We preliminarily identified the crystals by direct observation with an optical microscope and then by X-ray powder diffraction analysis. Some were also observed and photographed in a scanning electron microscope (SEM) JEOL JSM 6400.

**X-ray Powder Diffraction.** We used the X-ray powder diffraction technique to analyze several aspects of the KNP structural study, such as identifying the KNP crystalline phase and some neighboring phases in the determination of the KNP crystallization region. The experiments were carried out with a D5000 Siemens X-ray powder diffractometer in a  $\theta$ - $\theta$  configuration using the Bragg-Brentano geometry and Cu K $\alpha$  radiation.

We also used this technique to study the evolution of the crystal cell parameters with temperature and the linear thermal expansion tensor of KNP. The equipment was the same, but with a high-temperature chamber (Anton-Paar HTK10 platinum ribbon heating stage). The X-ray powder diffraction patterns were recorded, with a scintillation detector, at  $2\theta = 10$ – $70^\circ$ , step size =  $0.03^\circ$ , step time = 5 s, and temperatures of 298, 323, 373, 473, 573, 673, and 773 K, with a delay time of 300 s before each recording.

For the phase transitions of the KNP, performing the heating and cooling of the sample using the same equipment, in this case, a Braun position sensitive detector (PSD) was added. The X-ray powder diffraction patterns were recorded at  $2\theta = 10$ – $70^\circ$ , and the measuring time per degree was 10 s. We performed two experiments. In the first one, we studied how the material evolved with temperature from room temperature to 1273 K. In the second one, we used a smaller temperature range (from room temperature to 523 K) to specifically study the phase transition reported in the literature.<sup>1</sup> For the first experiment, we first heated the sample at a rate of 10 K/s from room temperature to 673 K, and then we

decreased the heating rate to 0.17 K/s and increased the temperature to 1273 K. From this maximum to room temperature, the same rates and temperature intervals were used. Diffraction patterns were registered every 50 K between 673 and 1273 K in both processes. For the second experiment, the sample was heated from room temperature to 373 K also at a rate of 10 K/s and between this temperature and 523 K at a rate of 0.017 K/s. We then performed the cooling process from 523 K to room temperature with the same rates and intervals and recorded the diffraction patterns in both processes every 25 K from 373 to 523 K.

#### Differential Thermal Analysis (DTA) Measurements.

We also studied the phase transitions of KNP by DTA measurements before studying them by X-ray powder diffraction. We used a TA Instruments simultaneous differential techniques instrument SDT 2960. The sample, which weighed around 20 mg, was placed in a platinum pan, and calcined Al<sub>2</sub>O<sub>3</sub> was used as reference material. We used Ar as purge gas at a flow of 90 cm<sup>3</sup>/min. We performed two experiments. In the first one, we used a heating rate of 10 K/min between room temperature and 1273 K, and in the second one, we used a heating rate of 1 K/min between room temperature and 523 K. The storage rate of data was always 0.5 s/data point.

**Top Seeded Solution Growth (TSSG).** To obtain KNP single crystals of a suitable size and quality for later optical studies, several growth experiments were carried out with the top seeded solution growth (TSSG)-slow cooling method without pulling. We used the same equipment as in the study of the crystallization region. The solution was placed in a platinum conical crucible of 25 cm<sup>3</sup>. The temperature was then increased to about 50 K above its saturation temperature and maintained for 3–4 h to homogenize the solution. The axial temperature gradient in the solutions was 0.75–0.92 K/mm, and the surface was colder than any other part of the solution. Crystals were grown with constant rotation using KNP parallelepipedic oriented seeds located at the center of the solution surface. The size of the seeds used was approximately constant for all growth experiences being  $10 \times 2 \times 2$  mm<sup>3</sup> along *a*, *b*, *c* with *a* disposed vertically or  $2 \times 10 \times 2$  mm<sup>3</sup> when *b* is disposed vertically to the solution surface.

We accurately determined the saturation temperature by observing the growth or dissolution of a KNP seed in contact with the surface of the solution. The crystals were grown submerged in the solution with constant rotation by decreasing the solution temperature at a rate of 0.1 K/h.

We studied three parameters of the KNP crystal growth process during the experiments: solution composition, seed orientation, and rotation velocity. These parameters and the results obtained are shown in Table 1 (see expts from 1 to 10).

These results led us to introduce a small change in the growth method in order to increase the mass transport in the solution and improve the quality of the KNP single crystals. We introduced a growth device previously tested in our laboratory.<sup>11</sup> To introduce it, we had to use a platinum conical

(11) Carvajal, J. J.; Nikolov, V.; Solé, R.; Gavaldà, Jna.; Massons, J.; Rico, M.; Zaldo, C.; Aguiló, M.; Díaz, F. *Chem. Mater.* **2000**, *12*, 3171.

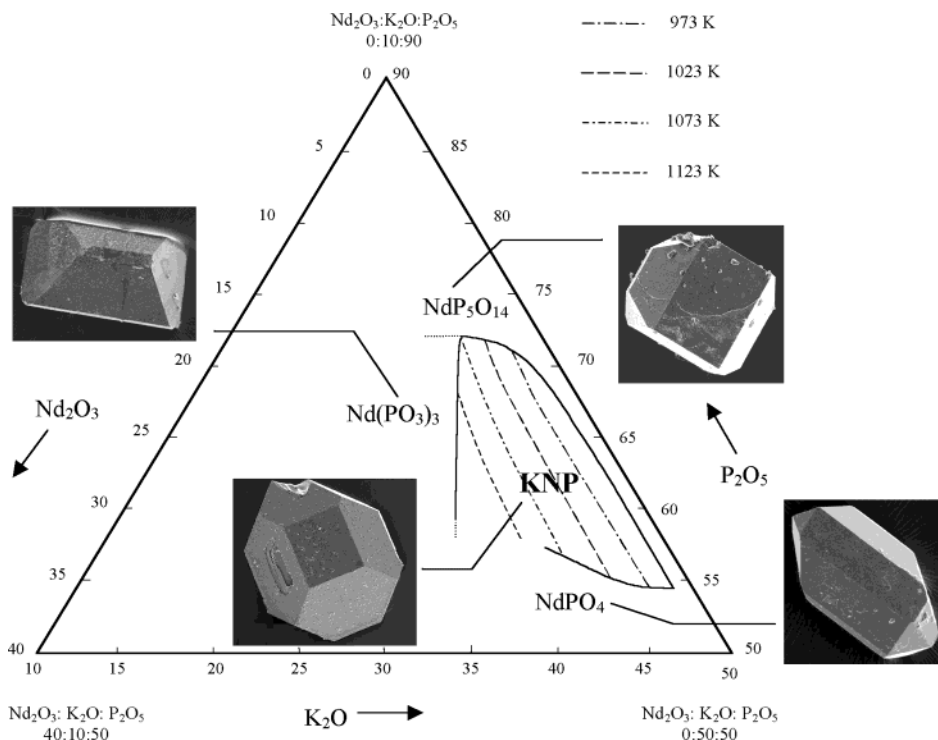


**Figure 1.** Crystallization Region of KNP and saturation temperatures in the system  $\text{Nd}_2\text{O}_3\text{-K}_2\text{O-P}_2\text{O}_5$ . SEM images of KNP and neighboring phases.

crucible of  $125\text{ cm}^3$ . This device comprises a platinum turbine, centered on the rotation axis, and two seed supports above it symmetrically displaced from this axis. With this device, we performed the two last experiments listed in Table 1. The growth parameters used were those that had provided the best results in the first study.

**Second Harmonic Generation (SHG) Measurements.** We used the Kurtz method<sup>12</sup> to measure the second harmonic response of the KNP. The sample analyzed was powdered and graded with standard sieves to obtain a uniform particle size, between 5 and  $20\ \mu\text{m}$ . After being packed uniformly, the sample was placed in a 2 mm-thick quartz cell and irradiated using a pulsed Nd:YAG laser.

We measured the energy reflected by the sample to estimate the incident power. We also measured the energy of the double radiation it emitted, which had double the frequency of the incident radiation, using a silicon PIN. The ratio between these signals was used to estimate the second harmonic efficiency of the sample. This ratio was calculated as an average of over 100 laser shots. This efficiency was compared with that of KDP,<sup>13</sup> which is a well-known nonlinear optical material.

## Results and Discussion

**KNP Crystallization Region.** The crystallization region of KNP in the  $\text{Nd}_2\text{O}_3\text{-K}_2\text{O-P}_2\text{O}_5$  system and the saturation temperature isotherms could be drawn after studying about 40 compositions of the solution. Figure 1 shows this crystallization region and some neighboring phases. It also shows SEM images of KNP and neighboring phases.

The crystallization region of KNP is placed between a  $\text{Nd}_2\text{O}_3/\text{K}_2\text{O}$  molar ratio of 25/75 and 3/97 and a  $\text{P}_2\text{O}_5$  concentration between 55 and 73 mol %. The saturation temperature isotherms are roughly parallel to the border of the crystallization region with the lowest

concentration of  $\text{Nd}_2\text{O}_3$ . This is also almost parallel to the isoconcentrational lines of this oxide. The saturation temperature isotherms increase from 973 to 1123 K when the  $\text{Nd}_2\text{O}_3$  molar ratio is also increased.

The neighboring phases of the crystallization region identified are  $\text{NdPO}_4$  (orthophosphate),<sup>14</sup>  $\text{Nd}(\text{PO}_3)_3$  (metaphosphate),<sup>15</sup> and  $\text{NdP}_5\text{O}_{14}$  (ultraphosphate).<sup>15</sup>  $\text{NdPO}_4$  crystallizes below the KNP crystallization region for a  $\text{P}_2\text{O}_5$  concentration of less than 55 mol %. In the same way,  $\text{NdP}_5\text{O}_{14}$  crystallizes above the KNP crystallization region for a  $\text{P}_2\text{O}_5$  concentration of more than 73 mol %. In the region between these two  $\text{P}_2\text{O}_5$  concentrations, and for a  $\text{Nd}_2\text{O}_3/\text{K}_2\text{O}$  molar ratio below 25/75, the  $\text{Nd}(\text{PO}_3)_3$  phase crystallizes. When the  $\text{Nd}_2\text{O}_3/\text{K}_2\text{O}$  molar ratio is above 3/97, the increase of the viscosity of the solution hinders the crystallization. Although the viscosity of the solution depends on its composition, it is very high throughout the crystallization region.

Crystal growth is difficult in highly viscous solutions. The molecules inside it have a low mobility so they find it difficult to reach the crystal surface. The average time of homogenization therefore increases, and the average growth rate and crystal quality decrease.

In this paper, we qualitatively studied the relationship between the solution composition and the growth rate, which is directly influenced by the viscosity of the solution. When we increased the  $\text{P}_2\text{O}_5$  concentration and kept the saturation temperature roughly constant, the viscosity of the solution went up. With this result, and taking into account the inverse relationship between viscosity and temperature, we chose a suitable zone of solution compositions in the crystallization region to initiate the crystal growth experiments and obtain high

(12) Kurtz, S. K.; Perry, T. T. *J. Appl. Phys.* **1968**, *39*, 3798.

(13) Dmitriev, V. G.; Gurzadyan, G. G.; Nikogosyan, D. N. *Handbook of Nonlinear Optical Materials*; Springer-Verlag: New York, 1991.

(14) Ni, X.-Y.; Hughes, J. M.; Mariano, A. N. *Am. Mineral.* **1995**, *80*, 21.

(15) Hong, H. Y.-P. *Acta Crystallogr.* **1974**, *B30*, 468.

quality KNP single crystals. The region that was apparently optimal for crystal growth is the one that has a low concentration of  $P_2O_5$  and the highest saturation temperature and also a high concentration of  $Nd_2O_3$ .

**Top Seeded Solution Growth (TSSG).** The experiments in which we analyzed the three growth parameters aforementioned in order to obtain information about the crystal growth of KNP are summarized in Table 1.

The effect of the seed orientation on the crystal growth was analyzed using  $Nd_2O_3-K_2O-P_2O_5 = 10/30/60$  as initial composition and a rotation velocity of 45 rpm (see experiments 1–3). We concluded that the  $a^*$  and  $b$  seed orientations were suitable for growing KNP single crystals. The crystal growth process (growth rate, quality) was similar using both of these orientations. On the other hand, the  $c^*$  orientation was unsuitable because when the crystal was heavy, the seed tended to break perpendicular to this direction, which led to a loss of crystal.

Four initial solution compositions were used in the study. Three of these,  $Nd_2O_3-K_2O-P_2O_5 = 10/30/60$  (expts 1–4), 7/31/62 (expt 5), and 6/34/60 (expts 7–12), were in the previously described optimum concentrations region and had low concentrations of  $P_2O_5$ , but one, 4/31/65 (expt 6), was fairly displaced from it and had a high concentration of  $P_2O_5$ . For experiment 6, the high viscosity of the solution due to the high  $P_2O_5$  concentration produced crystals that were too small and too light, despite the long cooling interval. The quality of the KNP single-crystal grown in this experiment was also too low. The growth processes with the other compositions (60 and 62  $P_2O_5$  mol %) were similar, but for the solution composition of 62  $P_2O_5$  mol % the growth rate was slightly lower and the average time of homogenization was slightly (about 2 or 3 h) longer.

The rotation velocity was also analyzed. Because the solution was very viscous, a high rotation velocity was needed. In fact, the quality of the crystals was best with the highest of the three rotation velocities we used (45, 60, and 75 rpm), and the growth rate increased slightly.

The quality of the single crystals grown was not sufficient, although it improved considerably when we used the final growth conditions (experiments 9 and 10) with the high rotation rate. We used the previously mentioned growth device. This increased the movement of the growth units inside the solution that had been hindered by its viscosity. The initial growth conditions used with the growth device are shown in Table 1 (experiments 11 and 12). The quality of the single crystals obtained was high. Figure 2a shows a KNP single-crystal grown using the conditions in experiment 11.

**Crystal Morphology of  $KNd(PO_3)_4$ .** To describe the morphology of the crystals, we observed KNP small single crystals by scanning electron microscopy (SEM) (Figure 1) and large single crystals using an optical microscope (Figure 2a). The habit was formed by the crystalline forms  $\{001\}$ ,  $\{100\}$ ,  $\{011\}$ ,  $\{0\bar{1}1\}$ ,  $\{110\}$ ,  $\{1\bar{1}0\}$ ,  $\{10\bar{1}\}$ ,  $\{1\bar{1}\bar{1}\}$ , and  $\{111\}$  (Figure 2b). Many of these faces are not equivalent by symmetry, but they are very similar, and it was difficult to identify them. Although KNP crystallizes in the monoclinic system, its  $\beta$  angle is close to  $90^\circ$ , and its cell parameters are quite

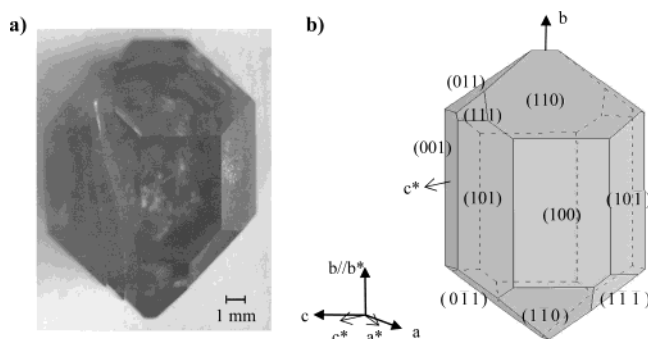


**Figure 2.** (a) KNP single crystal grown with a seed in the  $a$  direction. (b) Scheme of the crystal morphology where both direct ( $a$ ,  $b$ ,  $c$ ) and reciprocal ( $a^*$ ,  $b^*$ ,  $c^*$ ) lattices are indicated.

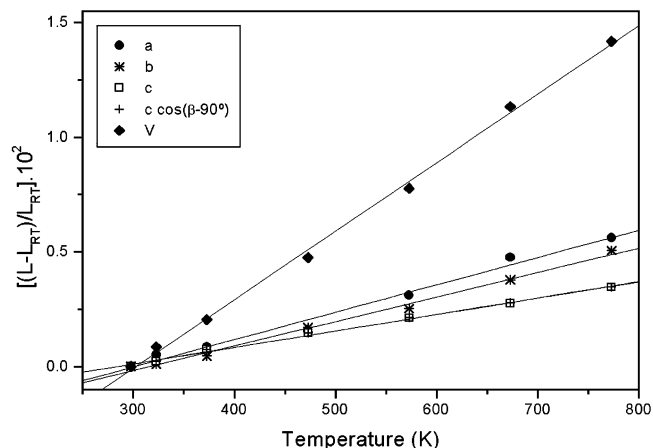


**Figure 3.** Relative thermal evolution of the cell parameters and unit cell volume of  $KNd(PO_3)_4$ .

similar. All these aspects made it difficult to identify the directions and faces of the single crystals by simple observation, so we used X-ray diffraction analysis in face indexation. It is very important to know the morphology of the crystal to be able to make its physical characterization.

**Linear Thermal Expansion Tensor.** As a monoclinic material, KNP shows crystallographic anisotropy in all its physical properties, such as its thermal expansion. When studying a laser material, it is very important to determine and locate the thermal ellipsoid because some of the pumping light power is converted into heat inside the crystal. In this paper, we have studied how the temperature affects the structure of the material.

We used X-ray powder diffraction in the 298–773 K temperature range to determine how the cell parameters evolved with temperature and then used the FULLPROF program<sup>16</sup> and the Rietveld method<sup>17</sup> to refine the cell parameters previously obtained. The linear relationship between the average change in each cell parameter ( $\Delta L/L$ ) and the temperature is shown in Figure 3. Cell parameters  $a$ ,  $b$ , and  $c$  increased as the temperature increased, but the  $\beta$  angle remained roughly constant. The increase was greatest in the  $[100]$  direction and lowest in the  $[001]$  direction. Although this

(16) Rodríguez-Carvajal, J. *Short Reference guide of the computer program FULLPROF*; Laboratoire León Brillouin, CEA-CNRS: Saclay, France, 1998.

(17) Young, R. A. *The Rietveld Method*; Oxford Science Publication, International Union of Crystallography: New York, 1995.

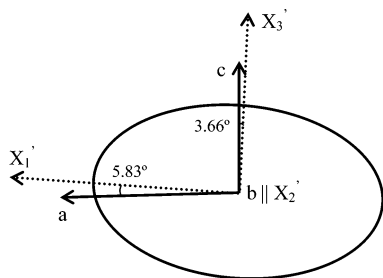


**Figure 4.** Thermal expansion ellipsoid for KNP in projection parallel to [010].

increase was low, KNP dilated slightly as the temperature increased. This is a good property for laser materials because they have to work at temperatures above room temperature.

The linear thermal expansion coefficients can be calculated from the slope of the linear relationship ( $\Delta L/L$ ) and the temperature for each unit cell parameter. The linear thermal expansion tensor at room temperature in the crystallophysical system  $X_1||a$ ,  $X_2||b$ ,  $X_3||c^*$  is

$$\alpha_{ij}(\text{KNP}) = \begin{pmatrix} 11.90 & 0 & 0.49 \\ 0 & 10.70 & 0 \\ 0.49 & 0 & 7.18 \end{pmatrix} \times 10^{-6} \text{ K}^{-1}$$

In the principal system,  $X_1'$ ,  $X_2' || b$ ,  $X_3'$ , the diagonalized linear thermal expansion tensor is

$$\alpha_{ij}'(\text{KNP}) = \begin{pmatrix} 11.95 & 0 & 0 \\ 0 & 10.70 & 0 \\ 0 & 0 & 7.13 \end{pmatrix} \times 10^{-6} \text{ K}^{-1}$$

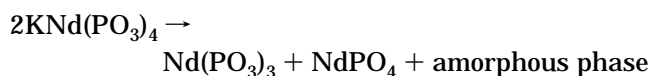
The principal axis with maximum thermal expansion,  $X_1'$ , was found 5.83° clockwise from the  $a$  axis. The axis with a minimum thermal expansion,  $X_3'$ , was found at 3.66° from the  $c$  axis. The thermal expansion ellipsoid in the principal axes is shown in Figure 4.

**Phase Transitions.** We used differential thermal analysis (DTA) and X-ray powder diffraction technique to study how the material evolved with temperature. The equipment used to do this analysis has already been described.

The stability of the KNP phase was analyzed between room temperature and 1273 K by differential thermal analysis and X-ray powder diffraction. The thermogram obtained in the 500–1250 K range is shown in Figure 5. An exothermic peak at 1165 K was observed. The change in weight during the experiment was not representative. We did a more detailed study using X-ray powder diffraction by heating and cooling the sample. At this temperature (1165 K), two new phases began to appear, but only one remained until room temperature. Figure 6 shows in the bottom the X-ray powder diffraction pattern of KNd(PO<sub>3</sub>)<sub>4</sub> at room temperature and the selected patterns at different temperatures describing the evolution of KNd(PO<sub>3</sub>)<sub>4</sub> with the temperature in both heating and cooling processes.

New peaks in the X-ray diffraction pattern recorded at 1173 K corresponded to these two phases. One was identified as Nd(PO<sub>3</sub>)<sub>3</sub> (70-0967-JPDS database<sup>18</sup>), and the other was identified as NdPO<sub>4</sub> (83-0654-JPDS database<sup>18</sup>). Although both of these phases appeared at

this temperature and almost at the same time they behaved differently. The intensity of the peaks for the Nd(PO<sub>3</sub>)<sub>3</sub> phase decreased steadily between 1173 and 1273 K, until they disappeared completely. On the other hand, the intensity of the peaks for the NdPO<sub>4</sub> phase increased steadily in the same temperature range and then remained fairly constant until the last X-ray diffractogram at room temperature in the cooling process. DTA and X-ray powder diffraction analysis showed that, at 1165 K, KNP decomposed irreversibly within weight loss into two new crystalline phases, Nd(PO<sub>3</sub>)<sub>3</sub> and NdPO<sub>4</sub>. However, between this temperature and 1273 K, a completely crystalline transformation of Nd(PO<sub>3</sub>)<sub>3</sub> into NdPO<sub>4</sub> occurred. The sample weight remained constant, so any amorphous phase was probably formed. X-ray powder diffraction analysis and DTA results suggested that the exothermic peak at 1165 K in the thermogram may be related to a decomposition of KNP in accordance with this reaction:



Under the measurement conditions, we used the phase transition at 440 K, reported in the literature<sup>1</sup> as a monoclinic-to-orthorhombic transition, which was not observed. To analyze this, we carried out a DTA study at lower velocity from room temperature to 523 K by heating and cooling the sample. We observed no phase transition at this temperature either in the heating cycle or the cooling cycle, though there was a very small change in weight, either in the heating cycle and the cooling cycle. We also analyzed this temperature range by X-ray powder diffraction and by heating and cooling the sample in the same temperature range and at the same rates. Again, no phase transition was observed.

**Second Harmonic Generation (SHG).** The SHG efficiency ( $\eta$ ) of KNP, calculated as described previously, was compared with the efficiency of KDP, which is widely used for nonlinear optical applications. The value of  $\eta/\eta_{\text{KDP}}$  we obtained was approximately one. The possibility that a self-frequency doubling laser may be developed increases the interest in this material.

## Conclusions

We determined the crystallization region of KNP in the Nd<sub>2</sub>O<sub>3</sub>–K<sub>2</sub>O–P<sub>2</sub>O<sub>5</sub> system with the saturation temperature isotherms and some neighboring phases. We chose a suitable region of compositions to perform the crystal growth, which is placed in the zone poor in P<sub>2</sub>O<sub>5</sub> and with high saturation temperatures, where the Nd<sub>2</sub>O<sub>3</sub> concentration is high.

We successfully grew KNP single crystals by the top seeded solution growth slow cooling method (TSSG). Crystal growth was optimized to achieve suitable quality and size of the crystals for later studies to check the applications of this material as miniaturized laser and nonlinear optical device.

KNP growth process have been studied and some growth parameters optimized. We have concluded that

(18) JCPDS-ICDD, Joint Committee for Powder Diffraction Standards-International Center for Diffraction Data: Philadelphia, PA, 2000.

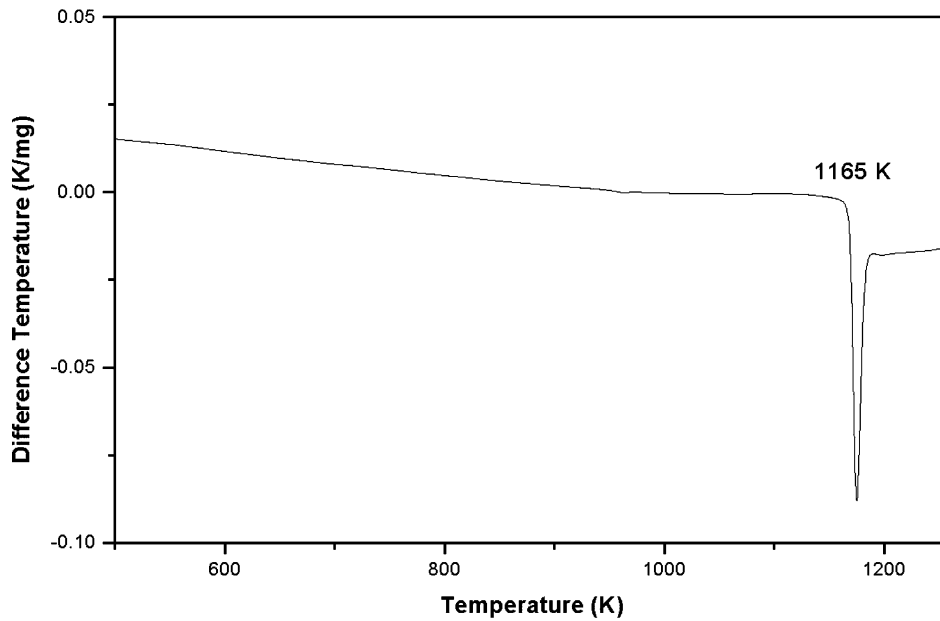


**Figure 5.** Differential thermal analysis (DTA) thermogram of  $\text{KNd}(\text{PO}_3)_4$  in the 573–1273 K temperature range.

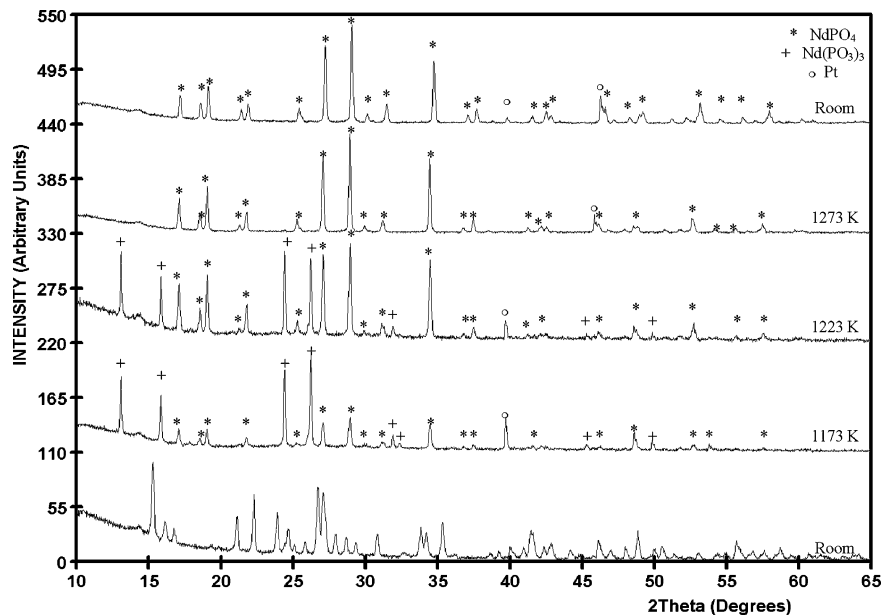


**Figure 6.** X-ray powder diffraction pattern of  $\text{KNd}(\text{PO}_3)_4$  at room temperature and the selected patterns at different temperatures describing the evolution of  $\text{KNd}(\text{PO}_3)_4$  with the temperature in both heating and cooling processes.

both  $a^*$  and  $b$  seed orientations are suitable for KNP growth by TSSG. For a  $c^*$  seed orientation, we have systematically lost the crystal. A low  $\text{P}_2\text{O}_5$  concentration is suitable for the growth process, which agrees with the conclusion we previously drew from the study of the crystallization region. We have also verified that a high rotation velocity facilitates crystal growth. The growth device we have used improves the quality of the crystals considerably.

We have also studied how the material behaved as the temperature increased. Phase transitions of the material have been determined. KNP decomposes irreversibly at 1165 K, according to the reaction proposed, thus generating two new crystalline phases  $\text{NdPO}_4$  and

$\text{Nd}(\text{PO}_3)_3$ . We have studied how the cell parameters evolved with the temperature and found that the material dilated slightly in any crystallographic direction.

Finally, since it may be used as nonlinear optical material, we measured the second harmonic efficiency of KNP, and this was similar to that of KDP.

**Acknowledgment.** The authors acknowledge financial support from DURSI 2001SGR317 and 2003FI00770 and CICyT MAT-02-04603-C05-03 and FIT070000-2002-461.

CM034812G